


Quantum-to-Classical Transition via Single-Shot Generalized Measurements

Zhenyu Xu 

School of Physical Science and Technology, Soochow University, Suzhou 215006, China

Quantum-to-classical transition for finite-dimensional systems is widely considered to occur continuously, yet the mechanism underlying the intermediate stage remains unclear. In this work, we address this challenge by adopting an operational framework to bridge discrete generalized coherent state positive-operator-valued measurements and continuous isotropic depolarizing channels. Our unified treatment reveals how dimensionality and decoherence rate collectively govern the quantum-to-classical transition. Notably, we demonstrate that a single-shot generalized measurement can eliminate most negative quasi-probabilities in phase space for finite-dimensional systems. Furthermore, we propose quantum circuit implementations achievable with current state-of-the-art quantum technologies.

Introduction—Decoherence and measurement exhibit a subtle interplay in explaining the quantum-to-classical transition [1–5]. The former describes how a quantum system gradually loses its quantum traits through interaction with the environment, leaving behind a few stable, classical-like states. The latter selects one of these possibilities and turns it into a definite outcome. These two processes together help explain how the classical world emerges from the underlying quantum reality. A positive-operator-valued measure (POVM) extends the standard framework of quantum measurement by using sets of positive operators that need not be mutually orthogonal [6]. POVMs are crucial for characterizing the statistics of measurements performed on subsystems of larger entangled states, and this formalism is inherently linked to decoherence [7]. They have broad applications ranging from quantum information science [8] and quantum metrology [9] to quantum field theory [10] and holographic black hole physics [11].

To explore the quantum-to-classical transition, a natural approach is to work in phase space [5]. In this framework, quasi-probability functions, which evolve under a generalized Liouville equation governed by the Moyal bracket, serve to establish analogies with classical dynamics. The appearance of negative values in quasi-probability functions within quantum phase space is often regarded as a hallmark of non-classicality, as such features have no counterpart in classical reality [12]. Quantum phase space formulations have attracted extensive attention, particularly in emerging quantum technologies [13], with recent applications spanning quantum foundations [14–22], quantum measurement theory [23, 24], and quantum chaos [25–27], among others.

It is widely accepted that the quantum-to-classical transition for finite-dimensional systems occurs gradually and continuously, yet the mechanism underlying the intermediate stage remains debated [1–5]. In this work, we address this fundamental question from the perspective of operational generalized measurements. We first demonstrate that n rounds of generalized N -level coherent state POVMs can be precisely represented by a continuous isotropic depolarizing channel. We further

establish a relationship connecting continuous decoherence evolution and discrete generalized measurements, revealing how increasing dimensionality or decoherence strength naturally transforms discrete measurements into continuous evolution. Crucially, our approach allows us to examine how initially minimal negative quasi-probability functions in phase space evolve under these POVMs. Remarkably, we find that a single round of such a measurement is sufficient to convert the most negative initial state into positive values for finite-dimensional systems, within certain quasi-probability representations. Finally, we provide an operational interpretation of this POVM construction and propose quantum circuit implementations that are compatible with current state-of-the-art quantum technologies.

N -level coherent state POVM—Without loss of generality, we consider a qudit, namely a quantum system with N distinguishable levels ($d = N$). The generalized N -level coherent state $|\Omega\rangle$ can be constructed in various ways [13, 28, 29]. In what follows, we employ the associated N -level coherent state POVM as

$$\int_{\mathcal{M}} E(\Omega) d\mu(\Omega) = \mathbb{1}_N, \quad (1)$$

where $E(\Omega) := N|\Omega\rangle\langle\Omega|$ denotes the element of POVMs, and $d\mu(\Omega)$ is the Haar measure on the manifold $\mathcal{M} = \text{SU}(N)/\text{U}(N-1) \cong \mathbb{CP}^{N-1}$, satisfying $\int_{\mathcal{M}} d\mu(\Omega) = 1$. Since $\text{Tr}[\rho E(\Omega)] = N\langle\Omega|\rho|\Omega\rangle \geq 0$ for any state ρ , the condition in Eq. (1) ensures that $E(\Omega)$ forms a valid POVM [7], defined as a set of positive semi-definite Hermitian operators that sum to the identity ($\mathbb{1}_N$). It is worth noting that, unlike the definition considered here, a related spin-coherent-state POVM was constructed for studying spin- J systems [30–32].

Here the N -level coherent state $|\Omega\rangle$ is parameterized by $2N-2$ angles with $0 \leq \theta_j \leq \pi$ and $0 \leq \phi_j \leq 2\pi$ ($j = 1, 2, \dots, N-1$), representing a generalization of the Bloch sphere. $|\Omega\rangle$ can be constructed by applying a unitary operator $U_N(\Omega) = \prod_{k=0}^{N-2} R_{k,k+1}(\theta_{k+1}, \phi_{k+1})$ to a ground state $|0\rangle_N = (1, 0, \dots, 0)^T \in \mathbb{C}^N$, namely, $|\Omega\rangle = U_N(\Omega)|0\rangle_N$ (or constructed recursively; see, for example, Ref. [29]). The rotational gate $R_{k,k+1}(\theta_{k+1}, \phi_{k+1}) =$

$\exp[-\frac{i\theta_{k+1}}{2}(\cos\phi_{k+1}X_{k,k+1} + \sin\phi_{k+1}Y_{k,k+1})]$ acts only the subspace $\{|k\rangle, |k+1\rangle\}$ and $X(Y)_{k,k+1}$ are the usual Pauli matrices. For example, when $N = 2$, $|\Omega\rangle = (\cos\frac{\theta_1}{2}, e^{i\phi_1}\sin\frac{\theta_1}{2})^T$, and when $N = 3$, $|\Omega\rangle = (\cos\frac{\theta_1}{2}, e^{i\phi_1}\sin\frac{\theta_1}{2}\cos\frac{\theta_2}{2}, e^{i(\phi_1+\phi_2)}\sin\frac{\theta_1}{2}\sin\frac{\theta_2}{2})^T$.

The initial density operator ρ_0 evolves under one round of POVM as $\mathcal{E}(\rho_0) = \int_{\mathcal{M}} d\mu(\Omega) M(\Omega) \rho_0 M(\Omega)^\dagger$, where $M(\Omega) := \sqrt{E(\Omega)} = \sqrt{N}|\Omega\rangle\langle\Omega|$ denotes the corresponding measurement operator. After some algebra, this yields $\mathcal{E}(\rho_0) = \mathbb{1}_N/N + (\rho_0 - \mathbb{1}_N/N)/(1+N)$. Thus, after n rounds of POVMs, the initial state evolves into (see Appendix A)

$$\rho_n = \underbrace{\mathcal{E} \circ \mathcal{E} \cdots \mathcal{E}}_n(\rho_0) = \frac{\mathbb{1}_N}{N} + \left(\frac{1}{N+1}\right)^n \left(\rho_0 - \frac{\mathbb{1}_N}{N}\right). \quad (2)$$

Clearly, as the number of measurement rounds increases, the final state asymptotically approaches the maximally mixed state, regardless of the initial state. Such behavior is reminiscent of a depolarizing channel in the context of decoherence theory [7]. In what follows, we justify this equivalence.

Generalized isotropic depolarizing channel—The standard GKSL master equation can be written as ($\hbar = 1$) [33, 34]

$$\frac{\partial \rho_t}{\partial t} = -i[H, \rho_t] + \sum_l \gamma_l \left(L_l \rho_t L_l^\dagger - \frac{1}{2} \{L_l^\dagger L_l, \rho_t\} \right), \quad (3)$$

where γ_l are a set of non-negative coefficients representing decoherence rates, and L_l are the Lindblad operators. Let $T_\nu (\nu = 1, 2, 3, \dots, N^2 - 1)$ be an orthonormal set of traceless Hermitian matrices serves as the generators of $\mathfrak{su}(N)$ Lie algebra [35], satisfying $\text{Tr}(T_\mu T_\nu) = \delta_{\mu\nu}/2$. We now introduce a generalized pure isotropic depolarizing channel by setting $L_\nu = T_\nu$ with a uniform decoherence rate $\gamma_\nu \equiv \gamma$, which leads to

$$\frac{\partial \rho_t}{\partial t} = \gamma \left(T_\nu \rho_t T_\nu - \frac{N^2 - 1}{2N} \rho_t \right) = \gamma \left(\frac{\mathbb{1}_N}{2} - \frac{N}{2} \rho_t \right), \quad (4)$$

where we have used $T_\nu T_\nu = \frac{N^2 - 1}{2N} \mathbb{1}_N$ [35] and the summation over repeated Greek indices is implicit. For the second equality in Eq. (4), we have employed $T_\nu X T_\nu = \text{Tr}(X) \mathbb{1}_N/2 - X/(2N)$ [35]. The solution for Eq. (4) is straightforward

$$\rho_t = \frac{\mathbb{1}_N}{N} + e^{-\frac{N}{2}\gamma t} \left(\rho_0 - \frac{\mathbb{1}_N}{N} \right). \quad (5)$$

Remarkably, by comparing Eq. (5) with Eq. (2), we find that setting

$$t = \frac{2n}{\gamma N} \ln(1+N), \quad (6)$$

yields an evolved state ρ_t that exactly matches ρ_n . This demonstrates that n rounds of N -level coherent state

POVMs are equivalent to evolution under the generalized isotropic depolarizing channel [36].

Equation (6) highlights the unification of continuous decoherence and discrete measurement descriptions. Let us examine two successive rounds of POVMs. The corresponding time interval is given by $\Delta t = 2 \ln(1+N)/(\gamma N)$. This implies that, for fixed decoherence rate γ , the time interval shrinks to an arbitrarily small value as the system dimension N increases. In other words, the discrete N -level coherent state POVMs process transitions smoothly into continuous decoherence dynamics in the large- N limit. For low-dimensional systems, however, this limit can only be reached if the decoherence rate γ is sufficiently large.

Quantum-to-classical transition in phase space—To investigate the quantum-to-classical transition, it is natural to work in phase space [5]. For discrete finite-dimensional quantum systems, the phase-space formalism was originally introduced by Stratonovich [37] and has been further developed over the past decades, particularly with the rise of quantum information and quantum technologies [13]. The key idea is to map an operator A in Hilbert space to an s -parametrized quasi-probability distribution function $W_A^s(\Omega)$ in the Ω -spanned phase space via the Stratonovich-Weyl kernel $\Delta^s(\Omega)$, namely,

$$W_A^s(\Omega) := \text{Tr}[A \Delta^s(\Omega)]. \quad (7)$$

For N -level quantum systems, such SW kernel can be constructed as $\Delta^s(\Omega) := \mathbb{1}_N/N + 4r_s R_\nu T_\nu$, where $R_\nu := \langle \Omega | T_\nu | \Omega \rangle$, and $r_s = \frac{1}{2} \sqrt{(N+1)^{1+s}}$ is the s -parametrized radius [29]. It is worth noting that although the parameter s is often taken as 0, 1, or -1 , analogous to the Cahill–Glauber s -parametrized quasiprobability distributions that yield the Wigner, P, and Q functions for continuous-variable systems [38, 39], it remains a free real parameter in N -level systems. In other words, $s \in \mathbb{R}$ can take any real value, as the corresponding SW kernel has been shown to satisfy the five essential criteria: linearity, reality, standardization, covariance, and trace preservation [40]. These properties ensure a valid and consistent SW correspondence [13]. Indeed, the freedom to choose s offers a powerful tool for deriving tight quantum speed limits in phase space [40] and optimizing the trade-off between speed and cost in shortcuts to adiabaticity, both theoretically and experimentally [41].

Equation (2) or (5) now in the phase space reads

$$W_{n(t)} = \frac{1}{N} + \Gamma_{n(t)} \left(W_0 - \frac{1}{N} \right), \quad (8)$$

with $\Gamma_n = 1/(1+N)^n$ and $\Gamma_t = e^{-\frac{N}{2}\gamma t}$, respectively. When no ambiguity is expected, here and throughout, we use $W_{n(t)}$ as a shorthand for $W_{\rho_{n(t)}}^s(\Omega)$ for simplicity. To explore the quantum-to-classical transition, we consider an initial quasi-probability distribution that attains a minimum (most negative) value (see Appendix

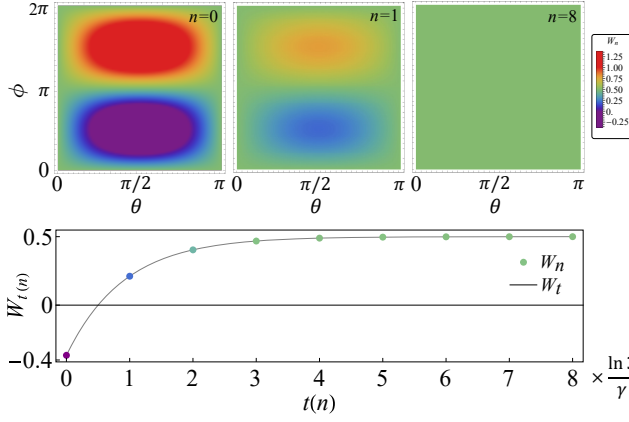


FIG. 1. **Quantum-to-classical transition via a single-shot POVM.** Top: The quasi-probability distribution function W_n (with $s = 0$) for a qubit after n rounds of two-level coherent state POVMs, where the POVM element is $E(\Omega) = 2|\Omega\rangle\langle\Omega|$ and the coherent state is given by $|\Omega\rangle = \cos \frac{\theta}{2}|0\rangle + \sin \frac{\theta}{2}e^{i\phi}|1\rangle$. Bottom: The equivalence between the coherent state POVM and the isotropic depolarizing channel. Both results demonstrate that a single round of POVM is sufficient to induce the transition from $W_0^{\min} < 0$ to $W_1 > 0$.

B), namely

$$W_0^{\min} = \frac{1}{N} - \frac{N-1}{N}(N+1)^{\frac{1+s}{2}}. \quad (9)$$

Equation (9) follows from $W_0 = \text{Tr}[\rho_0 \Delta^s(\Omega)] = 1/N + 2r_s R_\nu b_\nu(0)$, where the initial state is given by $\rho_0 = \mathbb{1}_N/N + b_\nu(0)T_\nu$, and $b_\nu(0) = 2 \text{Tr}(\rho_0 T_\nu)$. Using $R_\nu R_\nu = (N-1)/(2N)$ and noting that $b_\nu(0)b_\nu(0) \leq 2(N-1)/N$, with equality attained when the initial state is pure. As seen from a geometric perspective, the minimum of W_0 , i.e., Eq. (9) is achieved when the vectors R_ν and $b_\nu(0)$ are anti-parallel and the initial state is pure. In addition, to ensure $W_0^{\min} < 0$, the parameter s must satisfy $s > s_{\min}(N)$, where $s_{\min}(N) = -1 - \frac{2 \ln(N-1)}{\ln(N+1)}$. We note that, to properly characterize the negativity-to-positivity transition in the quasi-probability distribution, the parameter s must be held fixed, since although comparisons across phase spaces with different s values are permissible, they lack physical significance.

The transition from negativity to positivity in the phase space function after at least n_c rounds of N -level coherent state POVMs, is determined by the following condition:

$$n \geq n_c := \max \left\{ 1, \left\lceil \frac{1+s}{2} + \frac{\ln(N-1)}{\ln(N+1)} \right\rceil \right\}, \quad (10)$$

with $[x]$ representing the smallest integer that is greater than or equal to x . For example, if we consider the most widely used $s = 0$ (Wigner phase space), the critical number reads

$$n_c = \begin{cases} 1, & N = 2 \text{ or } 3, \\ 2, & N \geq 4, \end{cases} \quad (11)$$

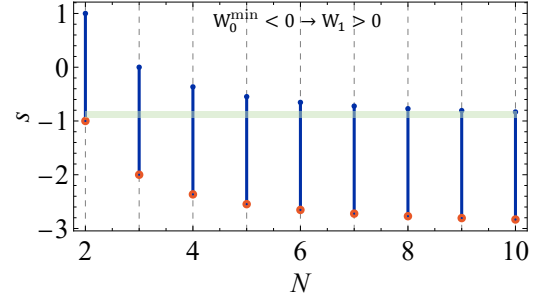


FIG. 2. **Conditions for single-shot transition from $W_0^{\min} < 0$ to $W_1 > 0$.** Blue regions indicate values of $s \in (s_{\min}(N), s_{\max}(N)]$ that allow a transition from negativity to positivity in the quasi-probability distribution after a single round of POVM, where $s_{\min}(N) = -1 - \frac{2 \ln(N-1)}{\ln(N+1)}$ and $s_{\max}(N) = 1 - \frac{2 \ln(N-1)}{\ln(N+1)}$. Red circles mark values that do not permit such a transition. Green regions denote choices of a fixed $s \in (-1, s_{\max}(N)]$ for which a one-shot transition can be realized across all finite N -level systems in such quasi-probability phase space.

which implies a single round of POVM already removes all negativity for qubits ($N = 2$) and qutrits ($N = 3$), while systems of dimension $N \geq 4$ need at least two rounds.

Example: Qubit case—For illustration, we consider the case $N = 2$, i.e., a qubit. When $s = 0$, we find that $n_c = 1$: a single round of two-level coherent state POVM is sufficient to eliminate the negativity of the phase space function, as evidenced in the top panels of Fig. 1, where the purple region vanishes after the measurement.

From the perspective of decoherence, this phenomenon is equivalent to the action of an isotropic depolarizing channel. For the qubit case, this is described by Eq. (4): $\frac{\partial \rho_t}{\partial t} = \frac{\gamma}{4} \sum_{l=x,y,z} (\sigma_l \rho_t \sigma_l - 3\rho_t)$, as shown in the bottom panel of Fig. 1, where the initial state in the phase-space is chosen to correspond to W_0^{\min} in Eq. (9). This panel illustrates the intermediate stages of the transition from two perspectives.

Conditions for single-shot transition—It is interesting to examine whether a single round ($n_c = 1$) of such generalized measurements can induce a transition from negativity to positivity in the quasi-probability distribution across systems of all finite dimensions ($N \neq \infty$). Indeed, we find that specific values of $s \in (s_{\min}(N), s_{\max}(N)]$ succeed, where $s_{\max}(N) = 1 - \frac{2 \ln(N-1)}{\ln(N+1)}$. For illustration, Fig. 2 highlights these regions with blue color. For example, when $N = 2$, $s = 0$ suffices, while for $N \geq 3$, $s = -1$ is effective.

Moreover, does there exist a specific quasi-probability phase space, i.e., a fixed s , such that all finite-dimensional systems can exhibit this transition through a single round of POVM? The answer is yes. Within the interval $s \in (-1, s_{\max}(N)]$ (highlighted by the green region in Fig. 2), there exists a range of s values for which a single round

of POVM ensures a transition from $W_0^{\min} < 0$ to $W_1 > 0$ for all finite N .

Experimental Proposal—The above theory can be directly implemented on state-of-the-art experimental platforms. Here, we briefly outline a feasible proposal for experimental verification, consisting of the following three steps.

Step 1—Haar measure on \mathbb{CP}^{N-1} . In the case of a rank-1 POVM such as $E(\Omega)$, the enlargement of the Hilbert space can effectively be substituted with classical randomness, eliminating the need for additional quantum resources. In other words, since $d\mu(\Omega) = \prod_{j=1}^{N-1} [p_j(\theta_j) d\theta_j \times \frac{d\phi_j}{2\pi}]$ [42], we can sample Ω by drawing each θ_j from $p_j(\theta_j) = (N-j) \sin^{2(N-j)-1}(\frac{\theta_j}{2}) \cos(\frac{\theta_j}{2})$, and each ϕ_j uniformly from $[0, 2\pi)$.

Step 2— N -level coherent state POVMs. The central task is to evaluate $\text{Tr}[\rho E(\Omega)]$, which can be implemented either probabilistically using ancilla-free continuous POVMs or deterministically with ancilla-assisted strategies. Since $|\Omega\rangle = U_N(\Omega)|0\rangle_N$, this can be realized by applying the inverse unitary $U_N^{-1}(\Omega)$ to ρ , performing a measurement in the computational basis, and post-selecting the outcome $|0\rangle_N$ (see in Fig. 3(a)). We note that $U_N(\Omega) = \prod_{k=0}^{N-2} R_{k,k+1}(\theta_{k+1}, \phi_{k+1})$, where each two-level rotation $R_{k,k+1}(\theta_{k+1}, \phi_{k+1})$ acts only on the subspace spanned by $\{|k\rangle, |k+1\rangle\}$. These rotations can be decomposed as $R_{k,k+1}(\theta_{k+1}, \phi_{k+1}) = R_z^{(k,k+1)}(\phi_{k+1} + \pi) R_y^{(k,k+1)}(\theta_{k+1}) R_z^{(k,k+1)}(-\phi_{k+1})$ (this decomposition is equivalent to the previously described formalism), where R_y and R_z denote standard single-qubit rotation gates embedded in the two-dimensional subspace. The advantage of this approach is that it requires no additional auxiliary qudits, although the success probability is limited to $1/N$.

For the latter approach, an ancilla qubit and a reference register are required, as illustrated in Fig. 3(b). We first sample Ω and prepare a second N -level register in the state $|0\rangle$. A single-qubit ancilla is initialized in $|0\rangle_A$ and subjected to a Hadamard gate. The key step is the application of a controlled-SWAP gate, $V_{\text{POVM}} = |0\rangle\langle 0|_A \otimes \mathbb{1}_{SR} + |1\rangle\langle 1|_A \otimes U_{\text{SWAP}}$, which conditionally exchanges the contents of the system S and the reference register R . A second Hadamard gate is then applied to the ancilla, followed by a measurement in the Pauli- Z basis. This yields the expectation value (see Appendix C) $\langle Z_A \rangle = \text{Tr}[\rho E(\Omega)]/N$, realizing the desired POVM. The advantage of this method is that it is deterministic and well-suited for low-dimensional systems, where the required ancilla and reference register resources remain feasible. This ancilla approach has been widely employed in both theory and experiment to explore a broad range of quantum phenomena. Applications include deterministic quantum computation with

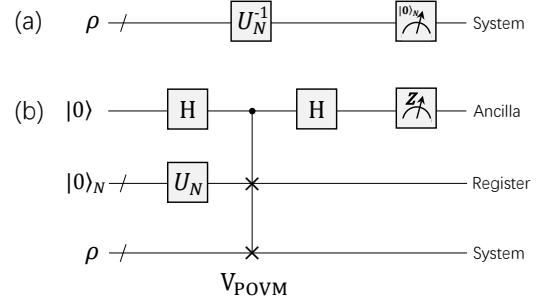


FIG. 3. Schematic quantum circuits for implementing N -level coherent state POVMs. (a) Direct measurement protocol via application of the inverse unitary U_N^{-1} , i.e., $\text{Tr}[U_N^{-1}\rho U_N|0\rangle_N\langle 0|] = \text{Tr}[\rho E(\Omega)]/N$. (b) Ancilla-assisted protocol for detecting the POVM using both an ancilla and a reference register. The key step involves a controlled-SWAP gate V_{POVM} between the system and the register. The outcome is obtained by measuring the ancilla in the Z basis, yielding $\langle Z_A \rangle = \text{Tr}[\rho E(\Omega)]/N$, which matches the result from (a) with 100% success probability at the cost of increased resource requirements.

a single pseudopure qubit [43], chaos and integrability testing [44–46], Loschmidt echoes [47, 48], work statistics [49–51], Lee-Yang zeros [52–54], full distributions of many-body observables [55], and the simulation of Hubbard model transitions [56], among others.

Step-3—Measure in phase space. In experiments, one may obtain the density matrix after performing the above POVM and directly use it to compute the phase-space function via Eq. (7). An alternative approach is to design digital quantum circuits to measure the function. The key idea is to construct the SW kernel using the linear combination of unitaries technique [57]. The phase-space function can then be recovered again using an ancilla-assisted method (see Appendix C).

Conclusions—We have explored the quantum-to-classical transition from an operational viewpoint by connecting discrete generalized N -level coherent state POVMs to continuous isotropic depolarizing channels. Our unified framework clarifies how dimensionality and decoherence strength bridge discrete measurements and continuous decoherence. Notably, we have demonstrated that even a single-shot measurement can completely remove the most negative phase space quasi-probability functions for finite-dimensional systems. We further propose quantum circuits tailored to current state-of-the-art quantum technologies for experimentally validating the theory. Our results provide insights into benchmarking the quantum-classical boundaries for finite-dimensional quantum systems and offer practical methods for managing the emergence of classicality via phase-space approaches. Additionally, our findings enable efficient simulation of open-system dynamics in quantum processors, particularly beneficial in platforms where direct noise modeling remains challenging [58].

Acknowledgements—This work was supported by the National Natural Science Foundation of China under Grant No. 12074280.

-
- [1] W. H. Zurek, Decoherence, einselection, and the quantum origins of the classical, *Rev. Mod. Phys.* **75**, 715 (2003).
 - [2] E. Joos, H. D. Zeh, C. Kiefer, D. Giulini, J. Kupsch, and I.-O. Stamatescu, *Decoherence and the Appearance of a Classical World in Quantum Theory*, 2nd ed. (Springer Berlin Heidelberg, Berlin, Heidelberg, 2003).
 - [3] M. Schlosshauer, Decoherence, the measurement problem, and interpretations of quantum mechanics, *Rev. Mod. Phys.* **76**, 1267 (2005).
 - [4] M. Schlosshauer, Quantum decoherence, *Physics Reports* **831**, 1 (2019).
 - [5] W. H. Zurek, *Decoherence and Quantum Darwinism: From Quantum Foundations to Classical Reality* (Cambridge University Press, 2025).
 - [6] E. B. Davies and J. T. Lewis, An operational approach to quantum probability, *Communications in Mathematical Physics* **17**, 239 (1970).
 - [7] M. A. Nielsen and I. L. Chuang, *Quantum Computation and Quantum Information*, 10th ed. (Cambridge University Press, Cambridge, UK, 2010).
 - [8] O. Gühne, E. Haapasalo, T. Kraft, J.-P. Pellonpää, and R. Uola, Colloquium: Incompatible measurements in quantum information science, *Rev. Mod. Phys.* **95**, 011003 (2023).
 - [9] V. Montenegro, C. Mukhopadhyay, R. Yousefjani, S. Sarkar, U. Mishra, M. G. Paris, and A. Bayat, Review: Quantum metrology and sensing with many-body systems, *Physics Reports* **1134**, 1 (2025).
 - [10] A. Peres and D. R. Terno, Quantum information and relativity theory, *Rev. Mod. Phys.* **76**, 93 (2004).
 - [11] T. Kibe, P. Mandayam, and A. Mukhopadhyay, Holographic spacetime, black holes and quantum error correcting codes: a review, *The European Physical Journal C* **82**, 463 (2022).
 - [12] T. L. Curtright, D. B. Fairlie, and C. K. Zachos, *A Concise Treatise on Quantum Mechanics in Phase Space* (World Scientific, 2014).
 - [13] R. P. Rundle and M. J. Everitt, Overview of the phase space formulation of quantum mechanics with application to quantum technologies, *Advanced Quantum Technologies* **4**, 2100016 (2021).
 - [14] T. Tilma, M. J. Everitt, J. H. Samson, W. J. Munro, and K. Nemoto, Wigner functions for arbitrary quantum systems, *Phys. Rev. Lett.* **117**, 180401 (2016).
 - [15] H. Zhu, Permutation symmetry determines the discrete wigner function, *Phys. Rev. Lett.* **116**, 040501 (2016).
 - [16] S. Deffner, Geometric quantum speed limits: a case for wigner phase space, *New Journal of Physics* **19**, 103018 (2017).
 - [17] B. Shanahan, A. Chenu, N. Margolus, and A. del Campo, Quantum speed limits across the quantum-to-classical transition, *Phys. Rev. Lett.* **120**, 070401 (2018).
 - [18] H. Le Jeannic, A. Cavallès, K. Huang, R. Filip, and J. Laurat, Slowing quantum decoherence by squeezing in phase space, *Phys. Rev. Lett.* **120**, 073603 (2018).
 - [19] J. E. Runeson and J. O. Richardson, Spin-mapping approach for nonadiabatic molecular dynamics, *The Journal of Chemical Physics* **151**, 044119 (2019).
 - [20] M. Oliva and O. Steuernagel, Dynamic shear suppression in quantum phase space, *Phys. Rev. Lett.* **122**, 020401 (2019).
 - [21] J. E. Runeson and J. O. Richardson, Quantum entanglement from classical trajectories, *Phys. Rev. Lett.* **127**, 250403 (2021).
 - [22] M. Jorquera Riera and L. Loveridge, Uncertainty relations relative to phase-space quantum reference frames, *Phys. Rev. A* **111**, L060201 (2025).
 - [23] E. Descamps, N. Fabre, A. Keller, and P. Milman, Quantum metrology using time-frequency as quantum continuous variables: Resources, sub-shot-noise precision and phase space representation, *Phys. Rev. Lett.* **131**, 030801 (2023).
 - [24] D. C. Brody, E.-M. Graefe, and R. Melanathuru, Phase-space measurements, decoherence, and classicality, *Phys. Rev. Lett.* **134**, 120201 (2025).
 - [25] Q. Wang and M. Robnik, Statistics of phase space localization measures and quantum chaos in the kicked top model, *Phys. Rev. E* **107**, 054213 (2023).
 - [26] R. Basu, A. Ganguly, S. Nath, and O. Parrikar, Complexity growth and the krylov-wigner function, *Journal of High Energy Physics* **2024**, 264 (2024).
 - [27] A. Pizzi, Quantum trails and memory effects in the phase space of chaotic quantum systems, *Phys. Rev. Lett.* **134**, 140402 (2025).
 - [28] Y. Yang, G. Chiribella, and G. Adesso, Certifying quantumness: Benchmarks for the optimal processing of generalized coherent and squeezed states, *Phys. Rev. A* **90**, 042319 (2014).
 - [29] J. E. Runeson and J. O. Richardson, Generalized spin mapping for quantum-classical dynamics, *The Journal of Chemical Physics* **152**, 084110 (2020).
 - [30] D. M. Appleby, Optimal measurements of spin direction, *International Journal of Theoretical Physics* **39**, 2231 (2000).
 - [31] J. Kofler and C. Brukner, Conditions for quantum violation of macroscopic realism, *Phys. Rev. Lett.* **101**, 090403 (2008).
 - [32] E. Shojaei, C. S. Jackson, C. A. Riofrío, A. Kalev, and I. H. Deutsch, Optimal pure-state qubit tomography via sequential weak measurements, *Phys. Rev. Lett.* **121**, 130404 (2018).
 - [33] V. Gorini, A. Kossakowski, and E. C. G. Sudarshan, Completely positive dynamical semigroups of n -level systems, *Journal of Mathematical Physics* **17**, 821 (1976).
 - [34] G. Lindblad, On the generators of quantum dynamical semigroups, *Communications in Mathematical Physics* **48**, 119 (1976).
 - [35] H. E. Haber, Useful relations among the generators in the defining and adjoint representations of $SU(N)$, *SciPost Phys. Lect. Notes*, 21 (2021).
 - [36] Constructing POVM elements directly from Kraus operators is sound, but it merely guarantees the existence of an abstract measurement with statistics given by $\text{Tr}(\rho E_j)$. By itself, however, it usually provides little insight into how the measurement is physically implemented or what observable is being probed, although in some special cases are indeed possible. Hence, we use the operational N -level coherent state POVM.
 - [37] R. L. Stratonovich, On distributions in representation

- space, *Sov. Phys. JETP* **4**, 891 (1957).
- [38] K. E. Cahill and R. J. Glauber, Ordered expansions in boson amplitude operators, *Phys. Rev.* **177**, 1857 (1969).
- [39] K. E. Cahill and R. J. Glauber, Density operators and quasiprobability distributions, *Phys. Rev.* **177**, 1882 (1969).
- [40] W. Meng and Z. Xu, Quantum speed limits in arbitrary phase spaces, *Phys. Rev. A* **107**, 022212 (2023).
- [41] J.-W. Zhang, J.-T. Bu, J. C. Li, W. Meng, W.-Q. Ding, B. Wang, W.-F. Yuan, H.-J. Du, G.-Y. Ding, W.-J. Chen, L. Chen, F. Zhou, Z. Xu, and M. Feng, Single-atom verification of the optimal trade-off between speed and cost in shortcuts to adiabaticity, *Phys. Rev. Lett.* **132**, 213602 (2024).
- [42] K. Zyczkowski and H.-J. Sommers, Induced measures in the space of mixed quantum states, *Journal of Physics A: Mathematical and General* **34**, 7111 (2001).
- [43] E. Knill and R. Laflamme, Power of one bit of quantum information, *Phys. Rev. Lett.* **81**, 5672 (1998).
- [44] D. Poulin, R. Laflamme, G. J. Milburn, and J. P. Paz, Testing integrability with a single bit of quantum information, *Phys. Rev. A* **68**, 022302 (2003).
- [45] B. Swingle, G. Bentsen, M. Schleier-Smith, and P. Hayden, Measuring the scrambling of quantum information, *Phys. Rev. A* **94**, 040302 (2016).
- [46] D. V. Vasilyev, A. Grankin, M. A. Baranov, L. M. Sieberer, and P. Zoller, Monitoring quantum simulators via quantum nondemolition couplings to atomic clock qubits, *PRX Quantum* **1**, 020302 (2020).
- [47] H. T. Quan, Z. Song, X. F. Liu, P. Zanardi, and C. P. Sun, Decay of loschmidt echo enhanced by quantum criticality, *Phys. Rev. Lett.* **96**, 140604 (2006).
- [48] J. Zhang, X. Peng, N. Rajendran, and D. Suter, Detection of quantum critical points by a probe qubit, *Phys. Rev. Lett.* **100**, 100501 (2008).
- [49] R. Dorner, S. R. Clark, L. Heaney, R. Fazio, J. Goold, and V. Vedral, Extracting quantum work statistics and fluctuation theorems by single-qubit interferometry, *Phys. Rev. Lett.* **110**, 230601 (2013).
- [50] L. Mazzola, G. De Chiara, and M. Paternostro, Measuring the characteristic function of the work distribution, *Phys. Rev. Lett.* **110**, 230602 (2013).
- [51] T. B. Batalhão, A. M. Souza, L. Mazzola, R. Auccaise, R. S. Sarthour, I. S. Oliveira, J. Goold, G. De Chiara, M. Paternostro, and R. M. Serra, Experimental reconstruction of work distribution and study of fluctuation relations in a closed quantum system, *Phys. Rev. Lett.* **113**, 140601 (2014).
- [52] B.-B. Wei and R.-B. Liu, Lee-yang zeros and critical times in decoherence of a probe spin coupled to a bath, *Phys. Rev. Lett.* **109**, 185701 (2012).
- [53] X. Peng, H. Zhou, B.-B. Wei, J. Cui, J. Du, and R.-B. Liu, Experimental observation of lee-yang zeros, *Phys. Rev. Lett.* **114**, 010601 (2015).
- [54] A. Francis, D. Zhu, C. Huerta Alderete, S. Johri, X. Xiao, J. K. Freericks, C. Monroe, N. M. Linke, and A. F. Kemper, Many-body thermodynamics on quantum computers via partition function zeros, *Science Advances* **7**, 2447 (2021).
- [55] Z. Xu and A. del Campo, Probing the full distribution of many-body observables by single-qubit interferometry, *Phys. Rev. Lett.* **122**, 160602 (2019).
- [56] X. Nie, X. Zhu, Y.-a. Fan, X. Long, H. Liu, K. Huang, C. Xi, L. Che, Y. Zheng, Y. Feng, X. Yang, and D. Lu, Self-consistent determination of single-impurity anderson model using hybrid quantum-classical approach on a spin quantum simulator, *Phys. Rev. Lett.* **133**, 140602 (2024).
- [57] N. W. Andrew M. Childs, Hamiltonian simulation using linear combinations of unitary operations, *Quantum Information and Computation* **12**, 0901 (2012).
- [58] J. Preskill, Quantum Computing in the NISQ era and beyond, *Quantum* **2**, 79 (2018)

Appendix A: Details for Eq. (2)

The measurement operator is defined by $M(\Omega) = \sqrt{E(\Omega)} = \sqrt{N}|\Omega\rangle\langle\Omega|$. Then, the density operator ρ after one POVM is given by

$$\mathcal{E}(\rho) = \int_{\mathcal{M}} d\mu(\Omega) M(\Omega) \rho M(\Omega)^\dagger = \int_{\mathcal{M}} N |\Omega\rangle\langle\Omega| \rho |\Omega\rangle\langle\Omega| d\mu(\Omega). \quad (\text{A1})$$

Assume $\rho = \frac{1}{N} \mathbb{1}_N + b_\nu T_\nu$, with $b_\nu = 2 \text{Tr}(\rho T_\nu)$, Eq. (A1) reads

$$\mathcal{E}(\rho) = \frac{1}{N} \mathbb{1} + \lambda b_\nu T_\nu, \quad (\text{A2})$$

where λ satisfies

$$\mathcal{E}(T_\nu) = \lambda T_\nu, \quad \text{or} \quad \lambda = \frac{2}{N^2 - 1} \text{Tr}(T_\nu \mathcal{E}(T_\nu)). \quad (\text{A3})$$

Submitting Eq. (A1) into Eq. (A3), we have

$$\lambda = \frac{2}{N^2 - 1} \int_{\mathcal{M}} N \text{Tr}[T_\nu |\Omega\rangle\langle\Omega| T_\nu |\Omega\rangle\langle\Omega|] d\mu(\Omega) = \frac{2N}{N^2 - 1} \int_{\mathcal{M}} \langle\Omega| T_\nu |\Omega\rangle^2 d\mu(\Omega). \quad (\text{A4})$$

Considering $\langle\Omega| T_\nu |\Omega\rangle^2 = \frac{1}{2} (1 - \frac{1}{N})$ (see proof of Eqs. (B2) and (B3) in Appendix B), we have

$$\lambda = \frac{1}{N + 1}. \quad (\text{A5})$$

Thus, the initial state $\rho_0 = \frac{1}{N} \mathbb{1}_N + b_\nu(0)T_\nu$ after one N -level coherent state POVM reads

$$\mathcal{E}(\rho_0) = \frac{\mathbb{1}_N}{N} + \lambda b_\nu^{(0)} T_\nu = \frac{\mathbb{1}_N}{N} + \frac{1}{N+1} \left(\rho_0 - \frac{\mathbb{1}_N}{N} \right), \quad (\text{A6})$$

and n rounds of POVMs

$$\rho_n = \frac{\mathbb{1}_N}{N} + \left(\frac{1}{N+1} \right)^n \left(\rho_0 - \frac{\mathbb{1}_N}{N} \right). \quad (\text{A7})$$

Appendix B: The minimum of W_0

To obtain the minimum (most negative) value of the initial quasi-probability distribution function, we first consider

$$W_0 = \text{Tr}[\rho_0 \Delta^s(\Omega)] = \frac{1}{N} + 2r_s R_\nu b_\nu(0), \quad (\text{B1})$$

where the SW kernel is given by $\Delta^s(\Omega) := \mathbb{1}_N/N + 4r_s R_\nu T_\nu$, $R_\nu := \langle \Omega | T_\nu | \Omega \rangle$, and $r_s = \frac{1}{2} \sqrt{(N+1)^{1+s}}$ is the s -parametrized radius [29]. The second equality in Eq. (B1) assumes the initial state is prepared in $\rho_0 = \frac{1}{N} \mathbb{1}_N + b_\nu(0)T_\nu$, with $b_\nu(0) = 2 \text{Tr}(\rho_0 T_\nu)$. Considering

$$\text{Tr}(\rho_0^2) = \frac{1}{N} + \frac{1}{2} b_\nu(0) b_\nu(0) \leq 1, \quad \text{i.e.,} \quad b_\nu(0) b_\nu(0) \leq \frac{2(N-1)}{N}, \quad (\text{B2})$$

the equality achieves when the initial state is pure.

On the other hand, we have

$$R_\nu R_\nu = \langle \Omega | T_\nu | \Omega \rangle^2 = [\text{Tr}(|\Omega\rangle\langle\Omega| T_\nu)]^2 = \frac{1}{4} (b_\nu(0) b_\nu(0))_{\max} = \frac{N-1}{2N}. \quad (\text{B3})$$

Therefore, the minimum of Eq. (B1) is obtained when the vector R_ν and $b_\nu(0)$ are opposite, namely

$$W_0^{\min} = \frac{1}{N} - \frac{N-1}{N} (N+1)^{\frac{1+s}{2}}. \quad (\text{B4})$$

In addition, Eq. (B4) can be negative if $s > -1 - 2 \ln(N-1)/\ln(N+1)$.

Appendix C: Details for the experimental proposal

1. Measurement protocol for $\text{Tr}[\rho_s E(\Omega)]$ with an ancilla

We employ an auxiliary qubit to probe the state of the system measured by the N -level coherent state POVM. The initial state is prepared in

$$\varrho_0 = |0\rangle\langle 0|_A \otimes \rho_S \otimes |\Omega\rangle\langle\Omega|_R. \quad (\text{C1})$$

Here, A , S , and R denote the auxiliary qubit, the system, and the reference register, respectively.

We then apply a Hadamard gate to the ancilla, yielding

$$\text{H} |0\rangle_A = \frac{1}{\sqrt{2}}(|0\rangle + |1\rangle)_A, \quad \varrho_1 = \frac{1}{2} \sum_{x,y \in \{0,1\}} |x\rangle\langle y|_A \otimes \rho_S \otimes |\Omega\rangle\langle\Omega|_R. \quad (\text{C2})$$

A controlled-SWAP gate $V_{\text{POVM}} = |0\rangle\langle 0|_A \otimes \mathbb{1}_{SP} + |1\rangle\langle 1|_A \otimes U_{\text{SWAP}}$ is then applied between the system and the reference register in the ancilla basis:

$$\varrho_2 = V_{\text{POVM}} \varrho_1 V_{\text{POVM}}^\dagger = \frac{1}{2} \begin{pmatrix} \rho_S \otimes P_R & (\rho_S \otimes P_R) U_{\text{SWAP}} \\ U_{\text{SWAP}} (\rho_S \otimes P_R) & P_S \otimes \rho_R \end{pmatrix}_A, \quad (\text{C3})$$

where

$$U_{\text{SWAP}} = \sum_{k,l=0}^{N-1} |l\rangle \langle k|_S \otimes |k\rangle \langle l|_P, \quad (\text{C4})$$

and

$$P_R = |\Omega\rangle \langle \Omega|_R, \quad P_S = |\Omega\rangle \langle \Omega|_S. \quad (\text{C5})$$

Finally, perform the second Hadamard gate and Z_A read-out on the ancilla, yielding

$$\langle Z_A \rangle = \text{Tr} \left[(Z_A \otimes \mathbb{1}_{SR}) (H \otimes \mathbb{1}_{SR}) \varrho_2 (H \otimes \mathbb{1}_{SR})^\dagger \right] = \text{Tr} [\rho_S |\Omega\rangle \langle \Omega|] = \text{Tr} [\rho_S E(\Omega)] / N. \quad (\text{C6})$$

2. Measurement protocol for $W_\rho^{(s)}(\Omega) = \text{Tr} [\rho \Delta^{(s)}(\Omega)]$

Since $\Delta^s(\Omega) := \mathbb{1}_N / N + 4r_s R_\nu T_\nu$ is not necessarily unitary, we can use the linear combination of unitaries technique [57]:

$$\Delta^{(s)}(\Omega) = \sum_{j=0}^{N^2-1} w_j U_j = w_0 U_0 + w_\nu U_\nu, \quad (\text{C7})$$

with $w_0 = 1/N$, $U_0 = \mathbb{1}_N$, $U_\nu = e^{-i\frac{\pi}{2}T_\nu}$ ($\nu = 1, \dots, N^2 - 1$), and $w_\nu = 4ir_s R_\nu$.

Then, we can introduce a register R of $m = \lceil \log_2 N^2 \rceil$ qubits prepared in

$$|\psi_R\rangle = \sum_{j=0}^{N^2-1} \sqrt{\frac{|w_j|}{\alpha}} |j\rangle, \quad \alpha = \sum_{j=0}^{N^2-1} |w_j|. \quad (\text{C8})$$

The controlled gate is given by

$$V_p = |0\rangle \langle 0| \otimes \mathbb{1} + |1\rangle \langle 1| \otimes U_p, \quad (\text{C9})$$

where

$$U_p = \sum_{j=1}^{N^2-1} |j\rangle \langle j|_R \otimes [\text{sgn}(w_j) U_j]. \quad (\text{C10})$$

Finally, we perform the Pauli-Z gate after the Hardmard gate on the ancilla, yielding

$$\langle Z \rangle = \text{Tr} [\rho \Delta^s(\Omega)] / \alpha. \quad (\text{C11})$$